Smart Structures and Systems, *Vol. 26, No. 1 (2020) 49-61*
DOI: https://doi.org/10.12989/sss.2020.26.1.049

Performance of multiple tuned mass dampers-inerters for structures under harmonic ground acceleration

Liyuan Cao, Chunxiang Li* and Xu Chen

Department of Civil Engineering, Shanghai University, No. 99 Shangda Road, Shanghai 200444, P.R. China

(*Received September 13, 2019, Revised March 30, 2020, Accepted April 9, 2020*)

Abstract. This paper proposes a novel high performance vibration control device, multiple tuned mass dampers-inerters (MTMDI), to suppress the oscillatory motions of structures. The MTMDI, similar to the MTMD, involves multiple tuned mass damper-inerter (TMDI) units. In order to reveal the basic performance of the MTMDI, it is installed on a single degree-of-freedom (SDOF) structure excited by the ground acceleration, and the dynamic magnification factors (DMF) of the structure-MTMDI system are formulated. The optimization criterion is determined as the minimization of maximum values of the relative displacement's DMF for the controlled structure. Based on the particle swarm optimization (PSO) algorithm to tune the optimum parameters of the MTMDI, its performance has been investigated and evaluated in terms of control effectiveness, strokes, stiffness and damping coefficient, inerter element force, and robustness in frequency domain. Meanwhile, further comparison between the MTMDI with MTMD has been conducted. Numerical results clearly demonstrate the MTMDI outperforms the MTMD in control effectiveness and strokes of mass blocks. Additionally, in the aspects of frequency perturbations on both earthquake excitations and structures, the robustness of the MTMDI is also better than the MTMD.

Keywords: high performance; dynamic magnification factors; optimization; structural vibration control; multiple tuned mass dampers-inerter; ground acceleration

1. Introduction

Vibrations of structures are mainly associated with resonances. When the frequency of a harmonic excitation matches the vibration frequency of a structure, dynamic amplification, which is largely dependent on the internal damping of the structure, will result in a vibration of large amplitude. In order to suppress these resonance-based vibrations, the internal damping of the structure can be increased by passive or active control technologies. In practical applications, passive control is a widely accepted method for structural control applications. The passive control devices include viscous dampers (VD), viscoelastic dampers (VED), tuned mass dampers (TMD), friction dampers (FD), and etc. A TMD is a mass–spring–dashpot system. By attaching a TMD to a structure, the vibration energy of the structure can be transferred to the TMD and dissipated via its dashpot. In recent decades, this type of TMD with low-cost and simple traits for structures have achieved significant success to reduce the vibration of slender flexible and low-damping structures, such as Taipei 101 Tower (508 m) in Taiwan (Chung *et al*. 2013), and Shanghai Tower (632 m) in Shanghai (Lu *et al*. 2017).

However, a major drawback of a single TMD is its sensitivity to the tuning frequency (Papadimitriou *et al*. 1997); that is, the TMD is not always robust. Robustness of the TMD is measured by mistuning, where the structural modal frequency to be controlled deviates from the frequency used for designing the TMD. Mistuning may be caused by errors identifying modal frequencies of the structure, perturbations of modal frequencies due to external excitations, as well as manufacturing errors of the TMD itself. Under the action of earthquakes, the effectiveness of a TMD depends on the relation between ground motions and the structural characteristics. For example, the investigations by Wang *et al*. (2005) and Anajafi and Medina (2018) demonstrated that if the structural predominant frequency were to locate within the bandwidth of the ground excitation spectrum, the TMD could consistently reduce the seismic responses of structures; however, if the external excitation frequencies were less than the structural fundamental frequency, the TMD effectiveness would decrease significantly. Therefore, it is not difficult to understand that up to now there is not a general agreement on the effectiveness of TMD in reducing the earthquake-induced responses of structures.

In order to increase the TMD robustness against mistuning effects in seismic scenarios, one of the feasible alternatives is to employ the multiple tuned mass dampers (MTMD) with distributed natural frequencies which have been investigated by, for example, Jangid (1995, 1999), Li (2000, 2002), Li and Liu (2003), Hoang and Warnitchai (2005), Han and Li (2008), Li and Ni (2007), Lin *et al*. (2010), Dehghan-Niri *et al*. (2010), Fu and Johnson (2011), Jokic *et al*. (2011), Daniel *et al*. (2012), Mohebbi *et al*. (2013), Daniel and Lavan (2014), Dinh and Basu (2015), Fadel Miguel *et al*. (2016), Lin *et al*. (2017), Zuo *et al*.

*Corresponding author, Professor,
E-mail: Li-chunxiang@vip.sina.com

ISSN: 1738-1584 (Print), 1738-1991 (Online)

(2017), Bozer and Özsarıyıldız (2018), and Tong and Zhao (2018). An MTMD system consists of multiple units of tuned mass dampers arranged in parallel, with each unit having its own mass, damping ratio, and natural frequency, thus owning the distributed natural frequencies. As such, for a structure with only one dominant vibration mode being needed to be controlled, an MTMD with natural frequencies distributed around this dominant frequency is more effective and more robust than a single TMD with an equal total mass. Furthermore, an MTMD is a viable solution to demanding small-sized TMDs owing to practical reasons, such as space limitations, transportation, and ease of handling.

On the other hand, the structural vibration suppression of using the inerter-based devices for has been a popular research topic since the first introduction of inerter in 2002 (Smith 2002). The inerter is a two terminal device, whose resisting force (called the inertance or apparent mass) is ideally proportional to the relative acceleration of its two terminals (Smith 2002); that is to say, it can supply a larger apparent mass of interest to the system to be connected. The apparent mass can be even 200 times higher than the physical mass of an inerter. Inertance is typically generated from the rotation of a flywheel, and there are four main types of inerter devices**:** rack and pinion inerter devices (Smith 2002, Lazar *et al*. 2014, Makris and Kampas 2016, Hessabi and Mercan 2016), ball and screw inerter devices (Hwang *et al*. 2007, Ikago *et al*. 2012, Garrido *et al*. 2013, Javidialesaadia and Wierschemb 2018), hydraulic inerter devices (Wang *et al*. 2010, Liu *et al*. 2018), and electromagnetic inerter devices (Nakamura *et al*. 2014, Gonzalez-Buelga *et al*. 2015, Takehiko *et al*. 2018). Aiming at more efficient energy dissipation, different inerter systems, including series layout inerter systems and series-parallel layout inerter systems have been investigated by, for example, Hu *et al*. (2015), Krenk and Høgsberg (2016), Pan *et al*. (2018), Pan and Zhang (2018), and Zhang *et al*. (2019). The greatest benefit of inerter is that it is able to produce a large apparent (effective) mass by using a relatively small rotational physical mass; therefore, the inerter is a possible solution to the issue that the performance of a conventional TMD is limited by the amount of mass in practical applications. Recently, the incorporation of an inerter into a TMD, named the tuned mass damper inerter (TMDI) was proposed by Marian and Giaralis (2014). Subsequently, the TMDI have been extensively investigated by, for example, Pietrosanti *et al*. (2017), Giaralis and Petrini (2017), Giaralis and Taflanidis (2018), Siami *et al*. (2018), Wen *et al*. (2017), Ruiz *et al*. (2018), Xu *et al*. (2019), and Cao and Li (2019). They all concluded that the TMDI, wherein the inerter is utilized as a mass amplifier to increase the inertial property of a TMD without increasing its weight, is a lower-mass and more effective alternative to a conventional TMD. Based on different arrangements of the TMD, inerter and base-isolation system, some novel hybrid control systems have been recently proposed by, for example, De Domenico and Ricciardi (2018a, b, c), and De Domenico *et al*. (2018) to surmount a few shortcomings, such as the large displacements concentrated at the isolation floor and the vulnerability to long-period ground motions. Likewise, at present, Inerter-based passive structural control has become more and more attractive for mitigating the dynamic responses of offshore wind turbine (Hu *et al*. 2018) and offshore platforms (Ma *et al*. 2018, 2019).

Based on the above review on both inerter and MTMD, although inerter has been applied in various mechanical systems, the application of inerter in the MTMD has not yet been reported. In the present paper, an inerter-based MTMD, referred to as the MTMDI has been, for the first time here, for attenuating undesirable oscillations of structures under the ground acceleration. Therefore, the specific work of the present study is to investigate and demonstrate the performance of the MTMDI by extensive simulation results based on the selected criteria for the optimality under the ground acceleration.

2. Formulations

2.1 DMFs of the structure MTMDI system

In this paper, the multiple tuned mass dampers-inerters (MTMDI) is recommended to attenuate the oscillatory motion of a single degree-of-freedom (SDOF) structure, effectively representing the main mode system in the specific vibration mode being controlled of multi-degrees-of-freedom (MDOF) structure, using mode reduced-order method. The main system is modeled by a mass m_s, a linear spring k_s, and a viscous damping c_s. Shown in Fig. 1, the MTMDI, similar to MTMD, involves multiple TMDI units, which is a classical TMD connected by an inerter device to the ground, and is installed on the SDOF system, excited by the ground acceleration $[\ddot{x}_g(t)]$. The equations of motion for the structure MTMDI system can then be expressed as

$$m_s\ddot{y}_s + c_s\dot{y}_s + k_s y_s = -m_s\ddot{x}_g + f_{MTMDI} \tag{1}$$

$$f_{MTMDI} = \sum_{j=1}^{n}\left[c_j(\dot{y}_j - \dot{y}_s) + k_j(y_j - y_s)\right] \tag{2}$$

$$\begin{aligned} m_j(\ddot{y}_j - \ddot{y}_s) + c_j(\dot{y}_j - \dot{y}_s) + k_j(y_j - y_s) \\ = -m_j\ddot{y}_s - m_j\ddot{x}_g - f_{Ij}, \\ j = 1, \quad 2, \quad \cdots, \quad n \end{aligned} \tag{3}$$

in which m_j, k_j, and c_j represent the mass, stiffness, and damping coefficient of the *j*th TMDI in the MTMDI, respectively; y_s and y_j denote the respective displacements of the structure and the *j*th TMDI in several with reference to the ground; f_{Ij} stands for the inerter element force corresponding to the inerter between the *j*th TMDI and the ground; *n* is the number of TMDIs.

In Fig. 1, the inerter device is described as a thick disk, which should be interpreted as an inertial weightless element and develop a resisting force proportioned to the relative acceleration of its terminals. The scale factor b_j, measured in mass unit, is known as the inertance coefficient of the inerter device in the *j*th TMDI. By the above

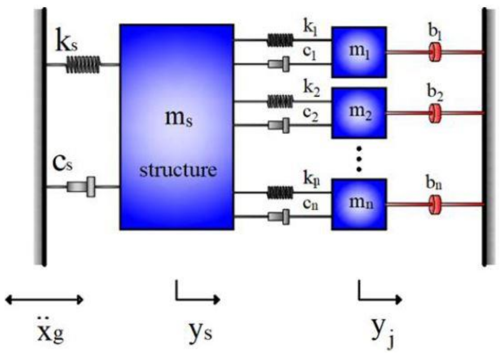

Fig. 1 Modeling of the structure-MTMDI system under the ground acceleration

description, the force f_{Ij} can be written as follows

$$f_{Ij} = b_j\left[\left(\ddot{x}_g + \ddot{y}_j\right) - \ddot{x}_g\right] \tag{4}$$

Laplace transforms of the displacement responses, ground acceleration, and resisting forces can be denoted, separately, as follows: $Y_s(s) = L[y_s(t)]$, $Y_j(s) = L\left[y_j(t)\right]$, $\ddot{X}_g(s) = L\left[\ddot{x}_g(t)\right]$, $F_{MTMDI}(s) = L[f_{MTMDI}(t)]$, $F_{Ij}(s) = L\left[f_{Ij}(t)\right]$. Then Eqs. (1)-(4) can be converted into the frequency domain forms by dint of the above Laplace transforms, and separately written as

$$\begin{aligned} &m_s s^2 Y_s(s) + c_s s Y_s(s) + k_s Y_s(s) \\ &= -m_s \ddot{X}_g(s) + F_{MTMDI}(s) \end{aligned} \tag{5}$$

$$\begin{aligned} F_{MTMDI}(s) = \sum_{j=1}^{n} \{ & c_j\left[sY_j(s) - sY_s(s)\right] \\ & + k_j\left[Y_j(s) - Y_s(s)\right]\} \end{aligned} \tag{6}$$

$$\begin{aligned} &m_j s^2\left[Y_j(s) - Y_s(s)\right] + c_j s\left[Y_j(s) - Y_s(s)\right] \\ &+k_j\left[Y_j(s) - Y_s(s)\right] \\ &= -m_j s^2 Y_s(s) - m_j \ddot{X}_g(s) - F_{Ij}(s) \\ &j = 1,\quad 2,\quad \cdots,\quad n, \end{aligned} \tag{7}$$

$$F_{Ij}(s) = b_j\left[\left(\ddot{X}_g(s) + s^2 Y_j(s)\right) - \ddot{X}_g(s)\right] \tag{8}$$

In order to get a normalized follow-up processing, we introduce the subsequent new variables

$$\omega_s = \sqrt{\frac{k_s}{m_s}},\quad \omega_j = \sqrt{\frac{k_j}{m_j}},\quad \xi_s = \sqrt{\frac{c_s}{2m_s\omega_s}},\quad \xi_j = \sqrt{\frac{c_j}{2m_j\omega_j}};$$
$$\mu = \frac{\sum_{j=1}^{n} m_j}{m_s},\quad \mu_j = \frac{m_j}{m_s},\quad \mu_I = \frac{\sum_{j=1}^{n} b_j}{m_s},\quad \mu_{Ij} = \frac{b_j}{m_j}.$$

Accordingly, the transfer functions, concerning the ground motion acceleration and the respective relative displacement responses and inertial forces of the structure with MTMDI, can readily be individually gotten as

$$G_s(i\omega) = \left.\frac{Y_s(s)}{\ddot{X}_g(s)}\right|_{s=i\omega}, \tag{9a}$$

$$G_j(i\omega) = \left.\frac{Y_j(s)}{\ddot{X}_g(s)}\right|_{s=i\omega}, \tag{9b}$$

$$G_{Ij}(i\omega) = \left.\frac{F_{Ij}(s)}{\ddot{X}_g(s)}\right|_{s=i\omega} \tag{9c}$$

where $i = \sqrt{-1}$, and ω is the circular frequency of external force. In the meantime, introducing dimensionless coefficients: $\lambda = \frac{\omega}{\omega_s}$ and $r_j = \frac{\omega_j}{\omega_s}$, the dynamic magnification factors (DMF) of respective relative displacements and inerter element forces of the structure and the jth TMDI in the MTMDI system can be expressed as follows

$$\begin{aligned} DMF_{Y_s} &= \left|\omega_s^2 G_s(i\omega)\right| \\ &= \left|-\frac{\bar{R}_e + \bar{I}_m i}{R_e + I_m i}\right| = \sqrt{\frac{\left[\bar{R}_e^2(\lambda) + \bar{I}_m^2(\lambda)\right]}{\left[R_e^2(\lambda) + I_m^2(\lambda)\right]}} \end{aligned} \tag{10}$$

$$\begin{aligned} DMF_{Y_j} &= \left|\omega_s^2 G_j(i\omega)\right| \\ &= \left|-\frac{\bar{R}_{ej} + \bar{I}_{mj} i}{R_{ej} + I_{mj} i}\right| = \sqrt{\frac{\left[\bar{R}_{ej}^2(\lambda) + \bar{I}_{mj}^2(\lambda)\right]}{\left[R_{ej}^2(\lambda) + I_{mj}^2(\lambda)\right]}} \end{aligned} \tag{11}$$

$$\begin{aligned} DMF_{F_{Ij}} &= \left|\frac{G_{Ij}(i\omega)}{m_s}\right| \\ &= \left|-\frac{\bar{R}_{eIj} + \bar{I}_{mIj} i}{R_{eIj} + I_{mIj} i}\right| = \sqrt{\frac{\left[\bar{R}_{eIj}^2(\lambda) + \bar{I}_{mIj}^2(\lambda)\right]}{\left[R_{eIj}^2(\lambda) + I_{mIj}^2(\lambda)\right]}} \end{aligned} \tag{12}$$

In which

$$R = \frac{r_j^2\left[r_j^2 - \lambda^2\left(1 + \mu_{Ij}\right)\right] + 4\xi_j^2 r_j^2 \lambda^2}{\left[r_j^2 - \lambda^2\left(1 + \mu_{Ij}\right)\right]^2 + 4\xi_j^2 r_j^2 \lambda^2},$$
$$I = \frac{2\xi_j r_j \lambda^3\left(1 + \mu_{Ij}\right)}{\left[r_j^2 - \lambda^2\left(1 + \mu_{Ij}\right)\right]^2 + 4\xi_j^2 r_j^2 \lambda^2},$$
$$\bar{R}_e(\lambda) = 1 + \sum_{j=1}^{n} \mu_j R,\qquad \bar{I}_m = -\sum_{j=1}^{n} \mu_j I,$$
$$R_e = (1 - \lambda^2) - \lambda^2 \sum_{j=1}^{n} \mu_j\left(1 + \mu_{Ij}\right) R,$$
$$I_m = 2\xi_s\lambda + \lambda^2 \sum_{j=1}^{n} \mu_j\left(1 + \mu_{Ij}\right) I;$$
$$\bar{R}_{ej}(\lambda) = R_e + \bar{R}_e r_j^2 - 2\xi_j r_j \lambda \bar{I}_m,$$
$$\bar{I}_{mj} = I_m + r_j^2 \bar{I}_m + 2\xi_j r_j \lambda \bar{R}_e,$$
$$R_{ej} = \left[r_j^2 - \lambda^2\left(1 + \mu_{Ij}\right)\right] R_e - 2\xi_j r_j \lambda I_m,$$
$$I_{mj} = \left[r_j^2 - \lambda^2\left(1 + \mu_{Ij}\right)\right] I_m + 2\xi_j r_j \lambda R_e;$$
$$\bar{R}_{eIj}(\lambda) = -\mu_j \mu_{IT} \lambda^2 \bar{R}_{ej},\qquad \bar{I}_{mIj} = -\mu_j \mu_{IT} \lambda^2 \bar{I}_{mj},$$
$$R_{eIj} = R_{ej},\qquad I_{mIj} = I_{mj}.$$

2.2 Configuration of the MTMDI

For the purpose of predigesting the fabrication of MTMDI, we hypothesize that the stiffness, damping coefficient, and inerter mass ratio of each TMDI in the

MTMDI are uniform (i.e., $k_j = k_T$, $c_j = c_T$, $\mu_{Ij} = \mu_{IT}$, $j = 1,\ 2,\ \cdots,\ n$), and the natural frequencies of the MTMDI are linearly distributed.

Subsequently, r_T and ξ_T are suggested to be the average frequency and damping ratio (i.e., $r_T = \sum_{j=1}^{n} \frac{r_j}{n}$ and $\xi_T = \sum_{j=0}^{n} \frac{\xi_j}{n}$) individually. Meanwhile, the non-dimensional parameter $\beta = \frac{(r_n - r_1)}{r_T}$ is defined as the frequency spacing of the MTMDI. In the light of the above definitions, the natural frequency of the jth TMDI is then expressed as

$$r_j = r_T\left[1 + \left(j - \frac{1+n}{2}\right)\frac{\beta}{n-1}\right] \tag{13}$$

According to the above hypothesis, the mass ratio, inerter mass ratio, and damping ratio of the jth TMDI in the MTMDI are, respectively, represented as

$$\mu_j = \frac{\mu}{r_j^2 \sum_{j=1}^{n} \frac{1}{r_j^2}} \tag{14}$$

$$\mu_{Ij} = \frac{\mu_I}{\mu} \tag{15}$$

$$\xi_j = \frac{r_j}{r_T}\xi_T \tag{16}$$

3. Optimum searching of the MTMDI

For the sake of protecting the civil engineering structures from devastation of earthquake, the present work concentrates on reducing their displace responses, basically guaranteeing the structural integrity and safety under external excitations. In actual research, a dimensionless value of the structure, namely dynamic magnification factors (DMF_{Y_S}) of its relative displacement, can be applied to measure performance of the MTMDI in the frequency domain. Naturally, the optimization goal is to minimize the maximum values of the DMF_{Y_S} with employing the particle swarm optimization (PSO) to search for the optimum parameters (i.e., r_T, β, and ξ_T listed on Table 1) by resorting to MATLAB software platform.

There are two procedures (PSO1 and PSO2) in the optimization process. The PSO2, used to search for the maximum of DMF_{Y_S} in the range from 0 to 2 of λ, is nested in PSO1, which serves for seeking the minimal $max.DMF_{Y_S}$ and its corresponding optimum parameters. At same time, the important parameters (i.e., population size, maximum and minimum weights, acceleration coefficients, maximum velocity, and end conditions) in the above PSO algorithms are shown in Fig. 2, the implementation flowchart of the PSO-based searching of the MTMDI.

In order to fully explore the property of the MTMDI,

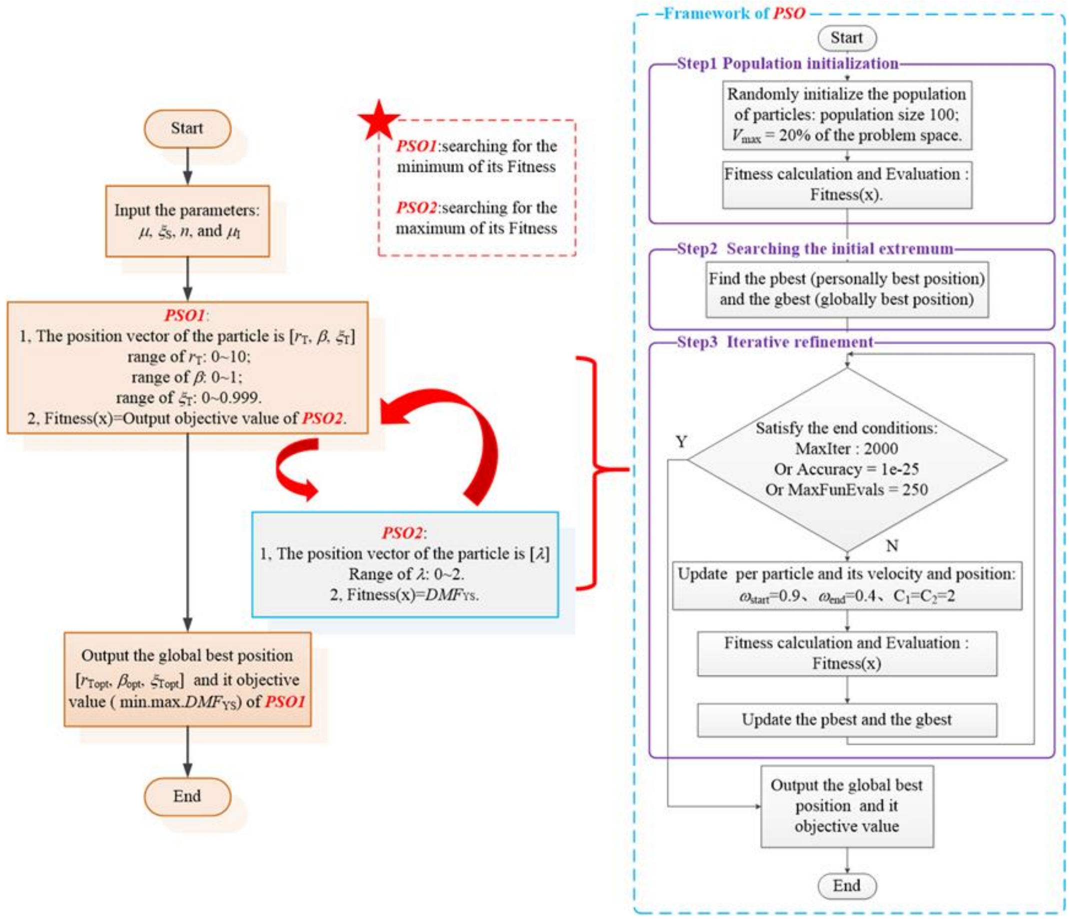

Fig. 2 Implementation flowchart of the PSO-based searching of the MTMDI

four models with various total mass ratio (μ) are studied, considering the different numbers of TMDIs (n). Furthermore, the value of total inerter mass ratio (μ_I) is varied in the range of 1-10% at intervals of 0.01 for the sake of a valuable insight into the sensitivity of the MTMDI to it. Noticeably, a careful comparison is made between the MTMDI with MTMD (i.e., the special case of the MTMDI with $\mu_I = 0$). Assigned values of the above parameters are presented in Table 1.

Table 1 Targets and ranges of explored parameters as well as assigned parameter values

Average frequency ratio	r_T (to be optimized)	$0 \le r_T \le 10$
Frequency spacing	β (to be optimized)	$0 \le \beta \le 1$
Average damping ratio	ξ_T (to be optimized)	$0 \le \xi_T \le 0.999$
Structural damping ratio	$\xi_s = 0.02$	
Total number of MTMDI	$n = 3, 7, 11, 15, 19$	
Total mass ratio	$\mu = 0.001,\ 0.005,\ 0.01,\ 0.05$	
Total inerter mass ratio	$\mu_I = 0,\ 0.01,\ 0.02,\ \dots,\ 0.1$	

4. Performance evaluation of the MTMDI

4.1 Control effectiveness

The three dimensional $max.DMF_{Y_s}^{\mathrm{opt}}$ surface is displayed in Fig. 3 used to estimate the effectiveness of the MTMDI concerning given ratio of the total inerter mass (μ_I) and number of TMDIs (n) under different total mass ratios (μ). From the trend and results shown in Fig. 3, there are some findings and suggestions as follow.

The $max.DMF_{Y_s}^{opt}$s of the MTMDI for each $\mu - n$ couple are always lower than that of the MTMD, and this decrease becomes particularly prominent when μ is 0.001. In this sense, the former has higher effectiveness than the latter, especially in the case of a smaller total mass. A probable explanation for this benefit is that installing the inerter devices equivalently puts on a virtual mass to the physical mass of the MTMD, and sequentially magnifies its inertia but without increasing physical mass. Moreover, the greater the total inerter mass ratio of the MTMDI, the better the control effectiveness. Therefore, by contrast, increasing the value of total inerter mass ratio can be accepted as a more expedient approach to enhance the effectiveness of the MTMDI than the addition of total mass ratio.

However, the variation curve of enhancement tendency for the control effectiveness becomes flatted as enlarging μ_I to more than 0.04, and increasing total inerter mass ratio inconspicuously improves the performance of vibration attenuation for the MTMDI in which case the μ equals to 0.05. A major reason for these phenomena is that in spite of the inertial enlargement as increasing either μ_I or μ, a biggish inertia will mitigate the oscillation of each block in the MTMDI, bringing out the dissipation saturation of energy for it. In consequence, from the economic perspective, the values of total mass ratio and total inerter mass ratio for the MTMDI are suggested to be within the ranges from 0.001 to 0.01 and 0.02 to 0.04, respectively, under which the MTMDI still keep an analogously preeminent control performance to one with $\mu = 0.05$.

Meanwhile, it is also visible from Fig. 3 that the control effectiveness of the either MTMD or MTMDI increases with the increase of n, but this sensibility of them (especial MTMDI) to n is quite weaker than to μ_I and μ. And if n is beyond 7, the value of their $max.DMF_{Y_s}^{\mathrm{opt}}$ is nearly invariable.

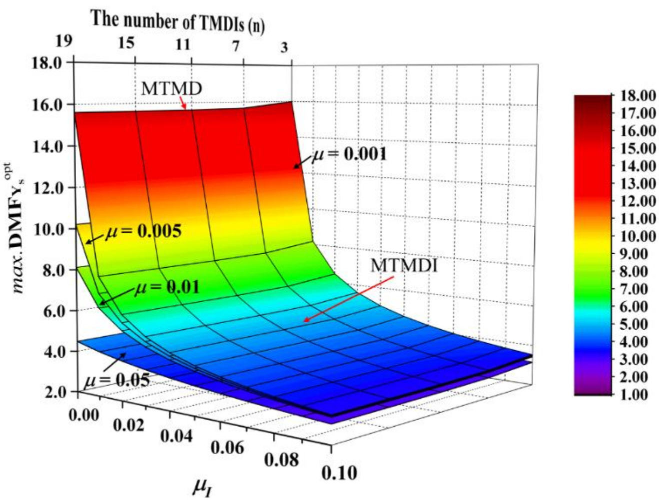

Fig. 3 Three-dimensional $max.DMF_{Y_s}^{\mathrm{opt}}$ surface used to estimate the effectiveness of the MTMDI concerning given ratio of the total inerter mass (μ_I) and number of TMDIs (n) under different total mass ratios (μ). $max.DMF_{Y_s}^{opt}$: the maximal dynamic magnification factor of the structure under the optimum parameters (f_{Topt}, β_{opt}, and ξ_{Topt})

4.2 Assessment of stroke

Every single ball, on the same line in Fig. 4, represents $max.DMF_{Y_j}$ of each TMDI in the MTMDI under the circumstances of the optimized parameters (r_{Topt}, ξ_{Topt}, and β_{opt}), utilized for the estimation of individual mass block's stroke.

It can be observed from Fig. 4, the stroke of each mass block in the MTMDI is remarkably smaller than that in the MTMD, particularly under a minor total mass ratio, and this preponderance is more excellent with increasing the total inerter mass ratio. However, as long as the total inerter mass ratio beyond 0.04 or the total mass ratio greater than or equal to 0.05, this reduction of the stroke in the MTMDI verges on the saturation. As obviously inferred, the stroke of each mass block greatly depends on its effective inertial mass, meaning that the larger the effective inertial mass, the smaller the stroke, which is why the MTMDI outperforms the MTMD under a same total mass ratio. The virtual mass, from the inerter, is proportionally far more than the physical mass of mass blocks under a small total mass ratio, and the virtue of the MTMDI is thus more obvious than the MTMD. And there is a sufficient effective inertial mass of the MTMDI under the total inerter mass ratio beyond 0.04 or the total mass ratio greater than or equal to 0.05, resulting in the reduction tendency toward saturation.

In addition, there are both similarities and differences between the MTMDI with MTMD from perspective of n. The uniformity is that the n of the either MTMDI or MTMD has a great effect on the stroke of each mass block. By increasing n, the strokes of the MTMDI and MTMD are enlarged and vice versa, but this variation tends to unnoticeable under n beyond 7. However, the disparity is that the strokes of the MTMD is, by and large, more sensitive to n than the MTMDI, in especial the total mass ratio is very small, that is one of weaknesses for the MTMD compared with the MTMDI.

4.3 Optimum stiffness and damping coefficient

Under the different total mass ratio (μ), the variation trends of both total and average optimal dimensionless stiffness ratios for the MTMDI with diverse number of TMDIs (n), concerning ratio of the total inerter mass (μ_I), are given in Fig. 5, and of both total and average optimum dimensionless damping coefficient ratios are given in Fig. 6.

From Fig. 5, the results indicate the total demand for stiffness of the MTMDI is higher than of the MTMD under a same total mass ratio, and increases with the growth of either μ or μ_I. It is noteworthy that these demands of the MTMDI and MTMD will be approximately equal if they have the same inertia. For instance, the values of $\frac{\sum k_j}{k_s}$ for the MTMDI under the circumstance of $\mu = 0.01$ and $\mu_I = 0.04$, and one for the MTMD with $\mu = 0.05$ are in several equal to 0.0458 and 0.0441, when n comes up to 7. Hence, based on the above phenomena, it can be speculated that the total inertia determines the total stiffness demand, that the bigger the former, the more the latter. As a result, a largish stiffness in the MTMDI gives rise to salient vibration mitigation of the mass blocks, in comparison with the MTMD under a same total mass ratio, which is the

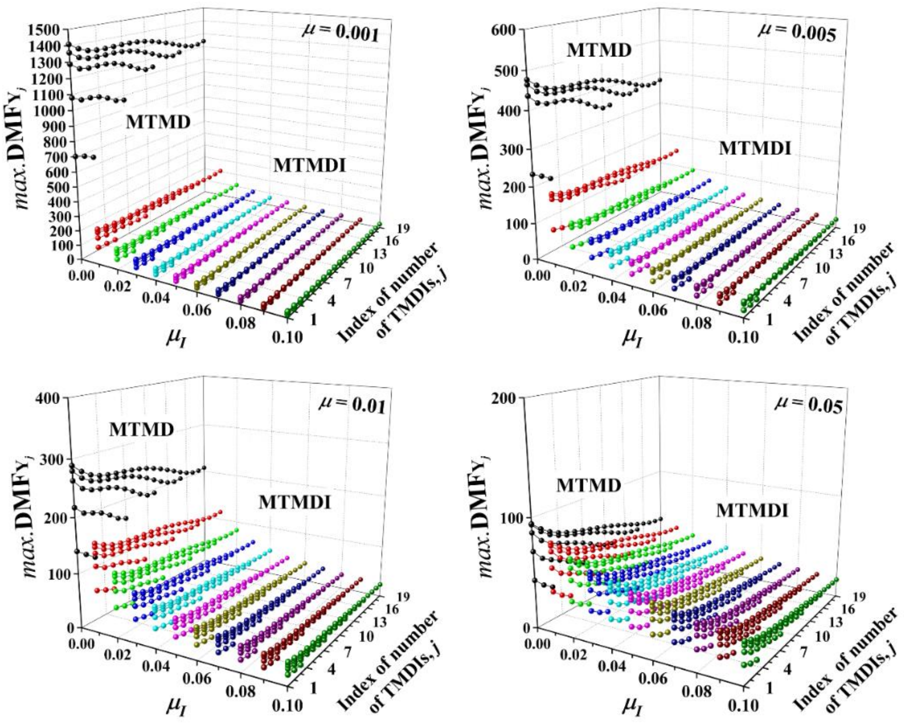

Fig. 4 Three-dimensional $max.DMF_{Y_j}$ point-and-line used to estimate the stroke of mass block of each unit in the MTMDI concerning given ratio of the total inerter mass (μ_I) and number of TMDIs (n) under different total mass ratios (μ)

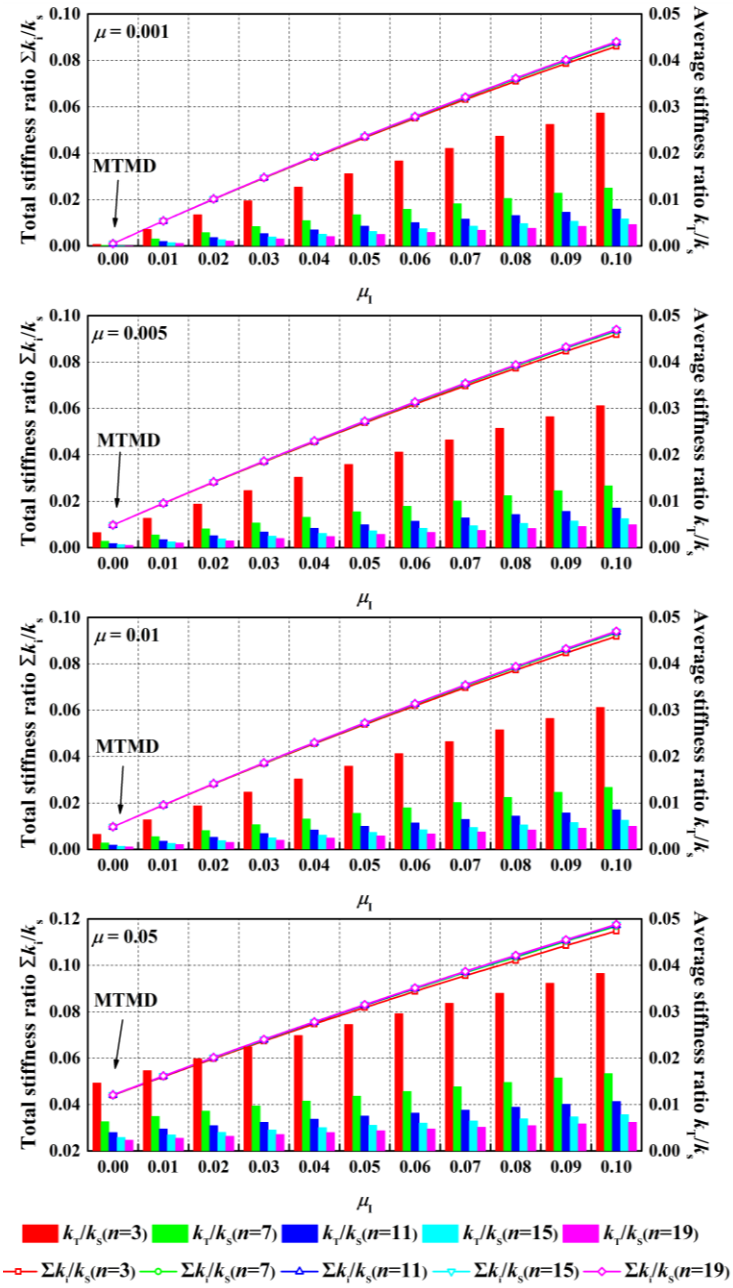

Fig. 5 Variation trends of both total and average optimal dimensionless stiffness ratios for the MTMDI with reference to ratio of the total inerter mass (μ_I) and number of TMDIs (n) under the under different total mass ratios (μ)

reason that MTMDI has a better stroke performance. Additionally, it can be further observed from Fig. 5 that the total stiffness is insensitive to the number of TMDIs. Based on this insensitivity, there is a smaller demand for the stiffness of each TMDI in the MTMDI with a bigger number of TMDIs, exactly as the trend of average stiffness with respect to n in Fig. 5.

Compared with the tendency of total stiffness, the similarity is the total damping coefficient in Fig. 6 raises remarkably as the quantity of the total inerter mass increases, but the difference is its decline with the augment of n in the MTMDI. Since a biggish damping can dissipate more energy, the aforementioned raise indicates a better dissipative capacity of the MTMDI than the MTMD, and this capacity is enhanced with the growth of μ_I. On account of the above-mentioned decrease of total damping coefficient with increasing n, the average damping coefficient of the MTMDI with n beyond 3 is strikingly smaller than that with n equal to 3, and the disparity between the MTMDI and the MTMD can be reduced by increasing n. In practice, the dashpot with a big damping coefficient is hard to implement, therefore, augmenting the number of TMDIs is a feasible way to gain a moderate damping for implementation.

4.4 Inerter element force

The graphs of the variation trends of $max.DMF_{F_{Ij}}$

with regard to total inerter mass ratio and number of TMDIs are shown in Fig. 7 to measure magnitude of the inerter element force in individual TMDI for the MTMDI. It can be observed that the inerter element force increases with the growth of the total inerter mass ratio, inversely decreases in the wake of augmenting the total mass ratio. Additionally, when the total inerter mass ratio outnumbers 0.04, this force gradually levels off. These phenomena indirectly reflect the service efficiency of the inerter element is higher when a small mass ratio than when a big one, and it is more economical for the total inerter mass ratio set to less than or equal to 0.04. Further discovering, on condition of adding the number of TMDIs, those variation phenomena tend to be not remarkable, excepting the diminution of individual inerter element force. Hence, an appropriate number of TMDIs not merely reduces the requirement of output force of the inerter element, but weaken its sensibility to the total mass ratio and total inerter mass ratio.

4.5 Robustness study

In engineering practice, the frequency characters of excitation and structure often influence the control performance of MTMD and MTMDI. Earthquake excitation contains luxuriant frequency components and thus amplifies the structural dynamic responses with its predominant frequency drawing near the natural frequency of the structure. Especially, there will be a sympathetic vibration to the structure when these two kinds of frequencies are equivalent. Employing the MTMDI, the suppression band-

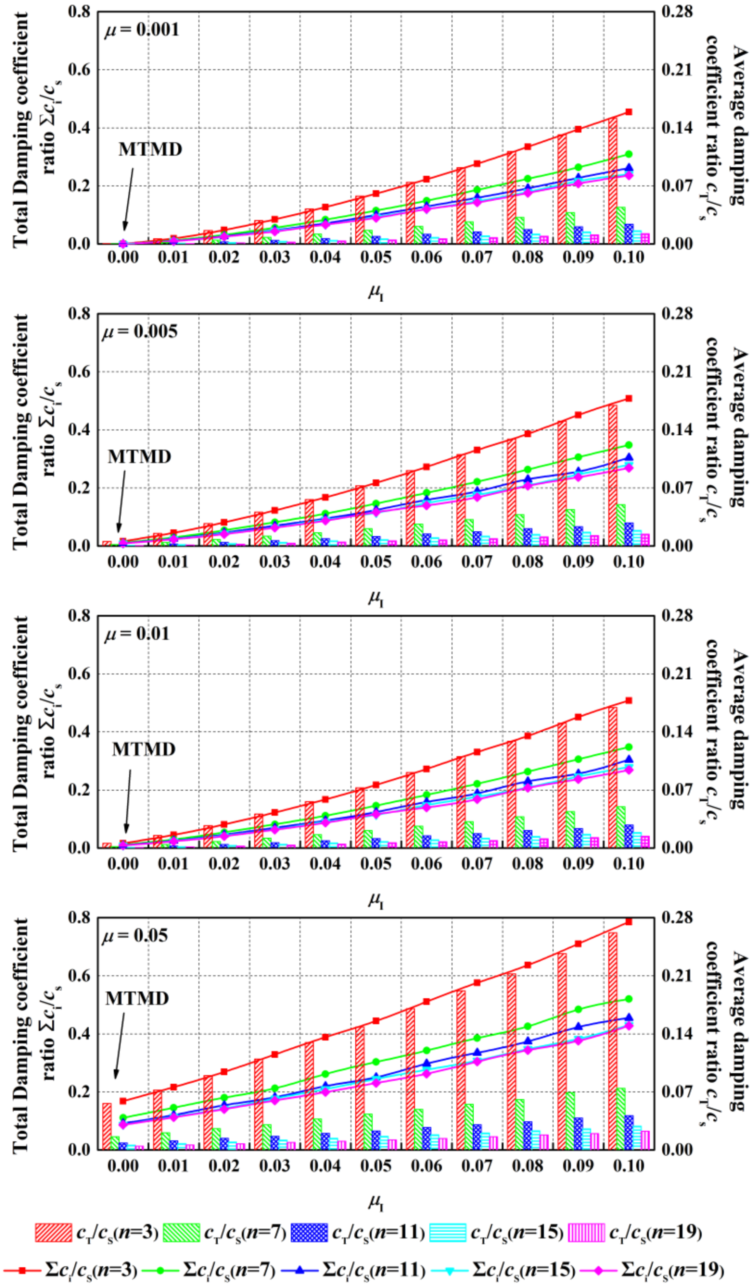

Fig. 6 Variation trends of both total and average optimal damping coefficient ratio for the MTMDI with reference to ratio of the total inerter mass (μ_I) and number of TMDIs (n) under the under different total mass ratios (μ)

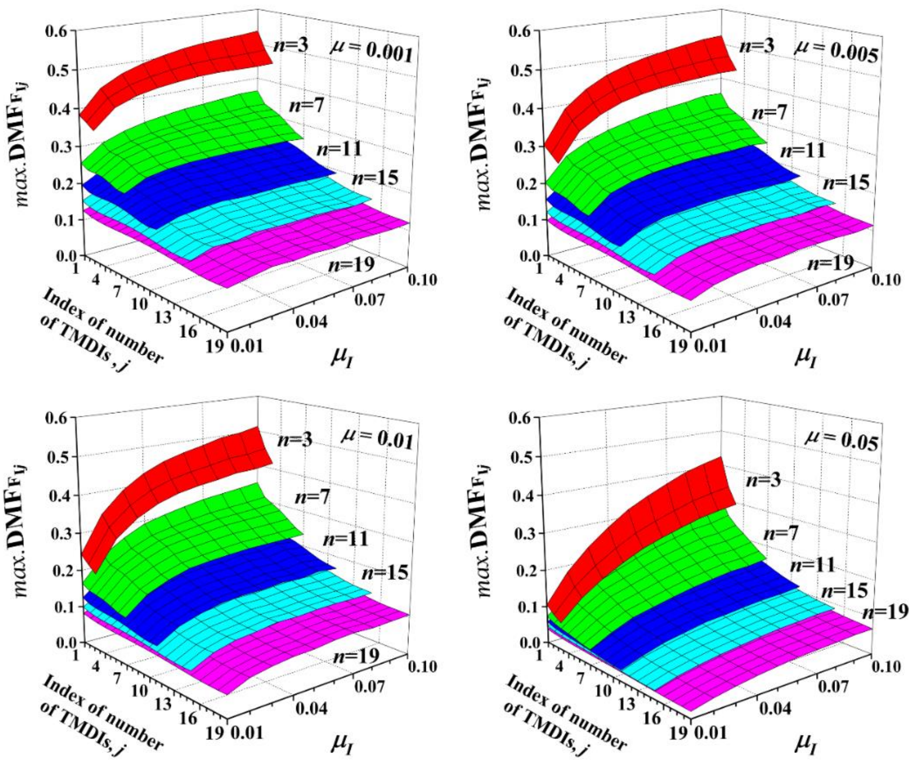

Fig. 7 Variation trends of the maximum $DMF_{F_{Ij}}$ of inerter element force in individual TMDI of the MTMDI with reference to ratio of the total inerter mass (μ_I) and number of units (n) under the under different total mass ratios (μ)

width (SB), the frequency range in which the structure controlled by the device outperforms an uncontrolled one (Garrido *et al*. 2013), is wider, thus meaning the device better faces to frequency change of the earthquake excitations. The DMF_{Y_s}s of the structure without and with the MTMDI and MTMD in frequency ratio range of 0.6-1.4 is shown in Fig. 8. Under the same $\mu = 0.01$ and $n = 7$, the SB of the MTMDI with $\mu_I = 0.04$ is markedly wider (about 90% wider) than that of the MTMD, which verifies that the MTMDI can effectively suppress the structural

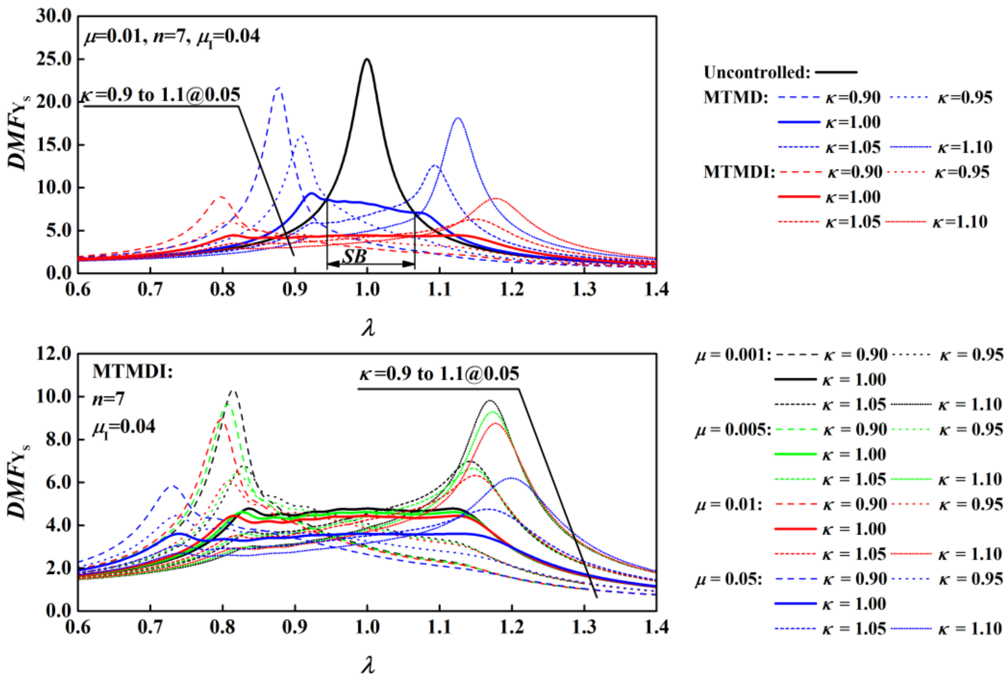

Fig. 8 Frequency response of the structure without and with the MTMDI and MTMD, DMF_{Y_s}: dynamic magnification factor of the structure

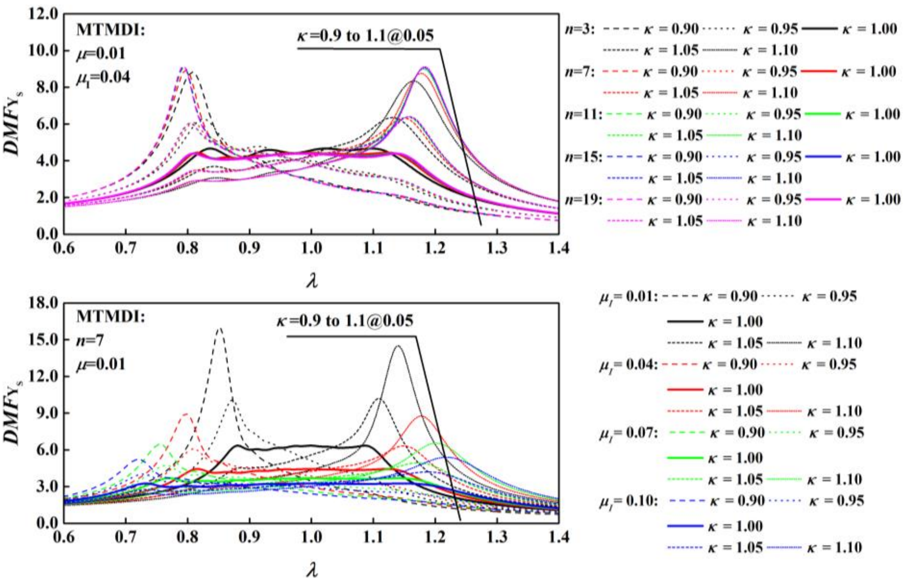

Fig. 8 Continued

Table 2 Suppression bandwidth (SB) of the MTMD and MTMDI under the circumstances of different total mass ratios, numbers of TMDIs, and total inerter mass ratios, respectively

		μ	n	μ_I	SB
MTMD		0.01	7		0.122
MTMDI	with the change of total mass ratio	0.001	7	0.04	0.215
		0.005			0.222
		0.01			**0.233**
		0.05			0.293
	with the change of number of TMDIs	0.01	3	0.04	0.227
			7		**0.233**
			11		0.237
			15		0.239
			19		0.239
	with the change of total inerter mass ratio	0.01	7	0.01	0.158
				0.04	**0.233**
				0.07	0.284
				0.10	0.324

response in a wider frequency range around resonance. And combined with Table 2, it can be visible that the enlargement of either total mass ratio or total inerter mass ratio greatly magnifies the SB for the MTMDI. In contrast, for five numbers of TMDIs, the values of SB are approximate, exce for flatter frequency-response curve with the increase of n.

With the exception of frequency perturbation on earthquake excitations, the perturbation of the structural frequency (Lin *et al*. 2017), due to errors identifying modal frequencies of the structure as well as nonlinear evolution of structures, also should be taken into account during the robustness study. In this work, κ ($\kappa = \frac{\omega_s^{'}}{\omega_s}$, $\omega_s^{'}$ is the perturbed frequency) is defined as the frequency ratio and changed from 0.9 to 1.10 as well as incremental interval, 0.05. The transformation tendency of peak for DMF_{Y_s} in Fig. 8 indicates that even the frequency of the structure varied around $\pm 10\%$ to the objective value, the MTMDI still can reduce the structural response to a greater extent than the MTMD. Additionally, the increase of either total mass ratio or total inerter mass ratio desensitize the $max.DMF_{Y_s}$ to the frequency perturbation of the structure. It is interesting that the larger the number of TMDIs, the rapider the rate at which $max.DMF_{Y_s}$ with the frequency perturbation ratio.

From the above, in comparison with MTMD, the robustness of the MTMDI is better by one tally, particularly enhancing it by increasing total inerter mass without the addition of physical mass for MTMDI. It is worth to be noted that the number of TMDIs for the MTMDI should not be too large from the robustness perspective, and is suggested as 7.

Beyond the above, Table 3 renders further comparison of total optimal dimensionless stiffness ratio and damping coefficient ratio, $max.DMF_{Y_s}^{opt}$, $max.DMF_{Y_j}$, and $max.DMF_{Y_{Ij}}$ of both the TMDI and MTMDI under unified total mass ratio ($\mu = 0.001$). It is a pleasure to discover that at an identical total mass ratio and total inerter mass ratio, not only can the MTMDI have a better control effectiveness, but also need a notably lesser total stiffness and damping coefficient than a single TMDI. According to tabular data, the former can be one tenth of the latter under the number of TMDIs for the MTMDI as 7. In spite of the increase of stroke, each TMDI for the MTMDI has a smaller inerter element force than for a single TMDI. Generally MTMDI have obvious advantages.

5. Conclusions

In this paper, a novel MTMDI system, involving

Table 3 Further comparison of total optimal dimensionless stiffness ratio and damping coefficient ratio, $max.DMF_{Y_s}^{opt}$, $max.DMF_{Y_j}$, and $max.DMF_{Y_{Ij}}$ of both the TMDI and MTMDI under unified total mass ratio ($\mu = 0.001$)

	μ_I	n	$\sum \frac{k_i}{k_s}$	$\sum \frac{c_i}{c_s}$	$max.DMF_{Y_s}^{opt}$	$max.DMF_{Y_j}$	$max.DMF_{F_{Ij}}$
TMDI	0.01	1	0.0107	0.0363	9.1790	65.4184	0.6120
	0.05		0.0455	0.3332	5.230	19.270	0.7991
MTMDI	0.01	3	0.0036	0.0063	8.1796	118.7924	0.3828
						113.9634	0.3698
						108.8744	0.3550
		7	0.0015	0.0018	7.8715	183.1715	0.2549
						174.5278	0.2438
						174.4502	0.2439
						173.1286	0.2419
						167.7136	0.2341
						160.6597	0.2244
						159.2843	0.2231
	0.05	3	0.0156	0.0578	4.6005	34.1518	0.5056
						31.2363	0.4715
						29.1297	0.4451
		7	0.0067	0.0165	4.3833	52.1633	0.3402
						47.9458	0.3156
						47.0334	0.3106
						45.9870	0.3034
						43.8696	0.2888
						41.3688	0.2727
						40.2236	0.2664

multiple units of TMDIs, has been recommended to mitigate the oscillatory motion of structures excited by the ground acceleration. Based on the particle swarm optimization algorithm to tune the optimum parameters of the MTMDI, the its performance has been investigated and evaluated in terms of control effectiveness, strokes, stiffness and damping coefficient, inerter element force, and robustness in frequency domain. Meanwhile, comparison between the MTMDI with MTMD has been conducted. The principal results and conclusions of this study can be drawn as:

(1) Benefitting from the inerter devices, the MTMDI is more effective than the MTMD and a single TMDI in attenuating the oscillation of structures.
(2) At equal total mass ratio, the stroke of each mass block for the MTMDI is remarkably smaller than that of the MTMD, depending on the virtual inertia from the inerter devices.
(3) In the context of a very small total mass ratio, the MTMDI still keeps a prominent advantage in the either control effectiveness or strokes, compared with the MTMD with a large mass ratio.
(4) In the aspects of frequency perturbations on both earthquake excitations and structures, the robustness of the MTMDI is also better than the MTMD.
(5) The number of TMDIs for the MTMDI is suggested to be 7 for the sake of reducing the requirements of stiffness, damping coefficient, and output inerter force for each TMDI for implementation, and meanwhile gaining a good robustness, while under which the MTMDI still keep a good performance of the control effectiveness and strokes.
(6) Based on the consideration of overall performance, practicability, and economy, the values of total mass ratio and total inerter mass ratio for the MTMDI are thus suggested to be within the ranges from 0.001 to 0.01 and 0.02 to 0.04, respectively.

Above all conclusions, it can be inferred that the MTMDI is a high performance vibration control device and has a good application prospect.

In closing, we present a little more detail on practical applications of the MTMDI for civil buildings. The proposed MTMDI can be applied to mitigate the vibration of MDOF structures under the ground acceleration. In these cases, each TMD in the MTMDI need to be placed simultaneously at the top floor of the structure, which is the location corresponding to maximum lateral displacement of an MDOF structure in general, and linked to one storey below the top floor of the structure or span more than one storey down by the respective inerter. Likewise, it can be anticipated that the more story the inerter spans down, the higher effectiveness the MTMDI achieves at reducing the structural vibration due to a larger acceleration increment. Moreover, in the seismic-isolated buildings, connecting the MTMDI to the isolation layer can bring out a prominent decrease of isolation layer lateral displacement without affecting its benefits to reduce seismic deformations of superstructure and bearings stability.

Acknowledgments

This study is supported by the National Natural Science Foundation of China (Grant No. 51978391).

References

Anajafi, H. and Medina, R.A. (2018), "Comparison of the seismic performance of a partial mass isolation technique with conventional TMD and base-isolation systems under broad-band and narrow-band excitations", *Eng. Struct.*, **158**, 110-123. https://doi.org/10.1016/j.engstruct.2017.12.018

Bozer, A. and Özsarıyıldız, S.S. (2018), "Free parameter search of multiple tuned mass dampers by using artificial bee colony algorithm", *Struct. Control Health Monit.*, **25**(2), e2066. https://doi.or g/10.1002/stc.2066

Cao, L. and Li, C. (2019), "Tuned tandem mass dampers-inerters with broadband high effectiveness for structures under white noise base excitations", *Struct. Control Health Monit.*, **26**(4), e2319. https://doi.org/10.1002/stc.2319

Chung, L.-L., Wu, L.-Y., Yang, C.-S.W., Lien, K.-H., Lin, M.-C. and Huang, H.-H. (2013), "Optimal design formulas for viscous tuned mass dampers in wind-excited structures", *Struct. Control Health Monit.*, **20**(3), 320-336. https://doi.org/10.1002/stc.496

Daniel, Y. and Lavan, O. (2014), "Gradient based optimal seismic retrofitting of 3D irregular buildings using multiple tuned mass dampers", *Comput. Struct.*, **139**, 84-97. https://doi.org/10.1016/j.compstruc.2014.03.002

Daniel, Y., Lavan, O. and Levy, R. (2012), "Multiple-tuned mass dampers for multimodal control of pedestrian bridges", *J. Struct. Eng. ASCE*, **138**(9), 1173-1178. https://doi.org/10.1061/(ASCE)ST.1943-541X.0000527

De Domenico, D. and Ricciardi, G. (2018a), "An enhanced base isolation system equipped with optimal tuned mass damper inerter (TMDI)", *Earthq. Eng. Struct. Dyn.*, **47**(5), 1169-1192. https://doi.org/10.1002/eqe.3011

De Domenico, D. and Ricciardi G. (2018b), "Improving the dynamic performance of base-isolated structures via tuned mass damper and inerter devices: A comparative study", *Struct. Control Health Monit.*, **25**, e2234. https://doi.org/10.1002/stc.2234

De Domenico, D. and Ricciardi, G. (2018c), "Optimal design and seismic performance of tuned mass damper inerter (TMDI) for structures with nonlinear base isolation systems", *Earthq. Eng. Struct. Dyn.*, **47**(12), 2539-2560. https://doi.org/10.1002/eqe.3098

De Domenico, D., Impollonia, N. and Ricciardi, G. (2018), "Soil-dependent optimum design of a new passive vibration control system combining seismic base isolation with tuned inerter damper", *Soil Dyn. Earthq. Eng.*, **105**, 37-53. https://doi.org/10.1016/j.soildyn.2017.11.023

Dehghan-Niri, E., Zahrai, S.M. and Mohtat, A. (2010), "Effectiveness-robustness objectives in MTMD system design: An evolutionary optimal design methodology", *Struct. Control Health Monit.*, **17**, 218-236. https://doi.org/10.1002/stc.297

Dinh, V.-N. and Basu, B. (2015), "Passive control of floating offshore wind turbine nacelle and spar vibrations by multiple tuned mass dampers", *Struct. Control Health Monit.*, **22**, 152-176. https://doi.org/10.1002/stc.1666

Fadel Miguel, L.F., Lopez, R.H., Miguel, L.F.F. and Torii, A.J. (2016), "A novel approach to the optimum design of MTMDs under seismic excitations", *Struct. Control Health Monit.*, **23**(11), 1290-1313. https://doi.org/10.1002/stc.1845

Fu, T.S. and Johnson, E.A. (2011), "Distributed mass damper system for integrating structural and environmental controls in buildings", *J. Eng. Mech. ASCE*, **137**(3), 205-213. https://doi.org/10.1061/(ASCE)EM.1943-7889.0000211

Garrido, H., Curadelli, O. and Ambrosini, D. (2013), "Improvement of tuned mass damper by using rotational inertia through tuned viscous mass damper", *Eng. Struct.*, **56**, 2149-2153. https://doi.org/10.1016/j.engstruct.2013.08.044

Giaralis, A. and Petrini, F. (2017), "Wind-induced vibration mitigation in tall buildings using the tuned mass-damper-inerter", *J. Struct. Eng. ASCE*, **143**(9), 04017127. https://doi.org/10.1061/(ASCE)ST.1943-541X.0001863

Giaralis, A. and Taflanidis, A.A. (2018), "Optimal tuned mass-damper-inerter (TMDI) design for seismically excited MDOF structures with model uncertainties based on reliability criteria", *Struct. Control Health Monit.*, **25**, e2082. https://doi.org/10.1002/stc.2082

Gonzalez-Buelga, A., Clare, L.R., Neild, S.A, Jiang, J.Z. and Inman, D.J. (2015), "An electromagnetic inerter-based vibration suppression device", *Smart Mater. Struct.*, **24**(5), 055015. https://doi.org/10.1088/0964-1726/24/5/055015

Han, B. and Li, C. (2008), "Characteristics of linearly distributed parameter-based multiple-tuned mass dampers", *Struct. Control Health Monit.*, **15**(6), 839-856. https://doi.org/10.1002/stc.222

Hessabi, R.M. and Mercan, O. (2016), "Investigations of the application of gyro-mass dampers with various types of supplemental dampers for vibration control of building structures", *Eng. Struct.*, **126**, 174-186. https://doi.org/10.1016/j.engstruct.2016.07.045

Hoang, N. and Warnitchai, P. (2005), "Design of multiple tuned mass dampers by using a numerical optimizer", *Earthq. Eng. Struct. Dyn.*, **34**(2), 125-144. https://doi.org/10.1002/eqe.413

Hu, Y.L., Chen, M.Z.Q., Shu, Z. and Huang, L.X. (2015), "Analysis and optimisation for inerter-based isolators via fixed-point theory and algebraic solution", *J. Sound Vib.*, **346**, 17-36. https://doi.org/10.1016/j.jsv.2015.02.041

Hu, Y., Wang, J., Chen, M.Z.Q., Li, Z.H. and Sun, Y. (2018), "Load mitigation for a barge-type floating offshore wind turbine via inerter-based passive structural control", *Eng. Struct.*, **177**, 198-209. https://doi.org/10.1016/j.engstruct.2018.09.063

Hwang, J.-S., Kim, J. and Kim, Y-M. (2007), "Rotational inertia dampers with toggle bracing for vibration control of a building structure", *Eng. Struct.*, **29**, 1201-1208. https://doi.org/10.1016/j.engstruct.2006.08.005

Ikago, K., Saito, K. and Inoue, N. (2012), "Seismic control of single-degree-of-freedom structure using tuned viscous mass damper", *Earthq. Eng. Struct. Dyn.*, **41**(3), 453-474. https://doi.org/10.1002/eqe.1138

Jangid, R.S. (1995), "Dynamic characteristics of structures with multiple tuned mass dampers", *Struct. Eng. Mech., Int. J.*, **3**(5), 497-509. https://doi.org/10.12989/sem.1995.3.5.497

Jangid, R.S. (1999), "Optimum multiple tuned mass dampers for base-excited undamped system", *Earthq. Eng. Struct. Dyn.*, **28**(9), 1041-1049. https://doi.org/10.1002/(SICI)1096-9845(199909)28:9<1041::AID-EQE853>3.0.CO;2-E

Javidialesaadia, A. and Wierschemb, N.E. (2018), "Optimal design of rotational inertial double tuned mass dampers under random excitation", *Eng. Struct.*, **165**, 412-421. https://doi.org/10.1016/j.engstruct.2018.03.033

Jokic, M., Stegic, M. and Butkovic, M. (2011), "Reduced-order multiple tuned mass damper optimization: A bounded real lemma for descriptor systems approach", *J. Sound Vib.*, **330** (22), 5259-5268. https://doi.org/10.1016/j.jsv.2011.06.005

Krenk, S. and Høgsberg, J.B. (2016), "Tuned resonant mass or inerter-based absorbers: unified calibration with quasi-dynamic flexibility and inertia correction", *Proc. R. Soc. A*, **472**(2185), 20150718. https://doi.org/10.1098/rspa.2015.0718

Lazar, I.F., Neild, S.A. and Wagg, D.J. (2014), "Using an inerter-based device for structural vibration suppression", *Earthq. Eng. Struct. Dyn.*, **43**(8), 1129-1147. https://doi.org/10.1002/eqe.2390

Li, C. (2000), "Performance of multiple tuned mass dampers for attenuating undesirable oscillations of structures under the ground acceleration", *Earthq. Eng. Struct. Dyn.*, **29**(9), 1405-1421. https://doi.org/10.1002/1096-9845(200009)29:9<1405::AID-EQE976>3.0.CO;2-4

Li, C. (2002), "Optimum multiple tuned mass dampers for structures under the ground acceleration based on DDMF and ADMF", *Earthq. Eng. Struct. Dyn.*, **31**(4), 897-919. https://doi.org/10.1002/eqe.128

Li, C. and Liu, Y. (2003), "Optimum multiple tuned mass dampers for structures under ground acceleration based on the uniform distribution of system parameters", *Earthq. Eng. Struct. Dyn.*, **32**(5), 671-690. https://doi.org/10.1002/eqe.239

Li, H.-N. and Ni, X.-L. (2007), "Optimization of non-uniformly distributed multiple tuned mass damper", *J. Sound Vib.*, **308**(1-2), 80-97. https://doi.org/10.1016/j.jsv.2007.07.014

Lin, C.-C., Wang, J.-F., Lien, C.-H., Chiang, H.-W. and Lin, C.-S. (2010), "Optimum design and experimental study of multiple tuned mass dampers with limited stroke", *Earthq. Eng. Struct. Dyn.*, **39**(14), 1631-1651. https://doi.org/10.1002/eqe.1008

Lin, C.-C., Lin, G.-L. and Chiu, K.-C. (2017), "Robust design strategy for multiple tuned mass dampers with consideration of frequency bandwidth", *Int. J. Struct. Stab. Dyn.*, **17**(1), 1750002. https://doi.org/10.1142/S021945541750002X

Liu, X., Jiang, J.Z., Titurus, B. and Harrison, A. (2018), "Model identification methodology for fluid-based inerters", *Mech. Syst. Signal Process.*, **106**, 479-494. https://doi.org/10.1016/j.ymssp.2018.01.018

Lu, X., Zhang, Qi, Weng, D., Zhou, Z., Wang, S., Mahin, S.A., Ding, S. and Qian, F. (2017), "Improving performance of a super tall building using a new eddy-current tuned mass damper", *Struct. Control Health Monit.*, **24**(3), e1882. https://doi.org/10.1002/stc.1882

Ma, R., Bi, K. and Hao, H. (2018), "Mitigation of heave response of semi-submersible platform (SSP) using tuned heave plate inerter (THPI)", *Eng. Struct.*, **177**, 357-373. https://doi.org/10.1016/j.engstruct.2018.09.085

Ma, R., Bi, K. and Hao, H. (2019), "A novel rotational inertia damper for heave motion suppression of semisubmersible platform in the shallow sea", *Struct. Control Health Monit.*, **26**, e2368. https://doi.org/10.1002/stc.2368

Makris, N. and Kampas, G. (2016), "Seismic protection of structures with supplemental rotational inertia", *J. Eng. Mech. ASCE*, **142**(11), 04016089. https://doi.org/10.1061/(ASCE)EM.1943-7889.0001152

Marian, L. and Giaralis, A. (2014), "Optimal design of a novel tuned mass-damper-inerter (TMDI) passive vibration control configuration for stochastically support-excited structural systems", *Probabilistic Eng. Mech.*, **38**, 156-164. https://doi.org/10.1061/(ASCE)EM.1943-7889.0001152

Mohebbi, M., Shakeri, K., Ghanbarpour, Y. and Majzoub, H. (2013), "Designing optimal multiple tuned mass dampers using genetic algorithms (GAs) for mitigating the seismic response of structures", *J. Vib. Control*, **19**(4), 605-625. https://doi.org/10.1177/1077546311434520

Nakamura, Y., Fukukita. A., Tamura, K., Yamazaki, I., Matsuoka, T., Hiramoto, K. and Sunakoda, K. (2014), "Seismic response control using electromagnetic inertial mass dampers", *Earthq. Eng. Struct. Dyn.*, **43**(4), 507-527. https://doi.org/10.1002/eqe.2355

Pan, C. and Zhang, R. (2018), "Design of structure with inerter system based on stochastic response mitigation ratio", *Struct. Control Health Monit.*, **25**(6), e2169. https://doi.org/10.1002/stc.2169

Pan, C., Zhang, R.F., Luo, H., Li, C. and Shen, H. (2018), "Demand-based optimal design of oscillator with parallel-layout viscous inerter damper", *Struct. Control Health Monit.*, **25**(1), e2051. https://doi.org/10.1002/stc.2051

Papadimitriou, C., Katafygiotis, L. and Au, S.K. (1997), "Effects of structural uncertainties on TMD design: A reliability-based approach", *Struct. Struct Control Health Monit.*, **4**(1), 65-88. https://doi.org/10.1002/stc.4300040108

Pietrosanti, D., De Angelis, M. and Basili, M. (2017), "Optimal design and performance evaluation of systems with tuned mass damper inerter (TMDI)", *Earthq. Eng. Struct. Dyn*., **46**(8), 1367-1388. https://doi.org/10.1002/eqe.2861

Ruiz, R., Taflanidis, A.A., Giaralis, A. and Lopez-Garcia, D. (2018), "Risk-informed optimization of the tuned mass-damper-inerter (TMDI) for the seismic protection of multi-storey building structures", *Eng. Struct.*, **177**, 836-850. https://doi.org/10.1016/j.engstruct.2018.08.074

Siami, A., Karimi, H.R., Cigada, A., Zappa, E. and Sabbioni, E. (2018), "Parameter optimization of an inerter-based isolator for passive vibration control of Michelangelo's Rondanini Pietà", *Mech. Syst. Signal Process*, **98**, 667-683. https://doi.org/10.1016/j.ymssp.2017.05.030

Smith, M.C. (2002), "Synthesis of mechanical networks: the inerter", *IEEE Trans. Autom. Contr.*, **47**(10), 1648-1662. https://doi.org/10.1109/TAC.2002.803532

Takehiko, A., Yoshikazu, A. and Kohju, I. (2018), "Structural control with tuned inertial mass electromagnetic transducers", *Struct. Control Health Monit.*, **25**, e2059. https://doi.org/10.1002/stc.2059

Tong, X. and Zhao, X. (2018), "Passive vibration control of the SCOLE beam system", *Struct. Control Health Monit.*, **25**, e2204. https://doi.org/10.1002/stc.2204

Wang, J.F., Lin, C.C. and Chen, B.L. (2005), "Vibration suppression for high-speed railway bridges using tuned mass dampers", *Int. J. Solids Struct.*, **42**(2), 465-491. https://doi.org/10.1016/S0020-7683(02)00589-9

Wang, F., Hong, M. and Lin, T. (2010), "Designing and testing a hydraulic inerter", *Proc. Inst. Mech. Eng. Part C: J. Mech. Eng. Sci.*, **225**(1), 66-72. https://doi.org/10.1243/09544062JMES2199

Wen, Y., Chen, Z. and Hua, X. (2017), "Design and evaluation of tuned inerter-based dampers for the seismic control of MDOF structures", *J. Struct. Eng. ASCE*, **143**(4), 04016207. https://doi.org/10.1061/(ASCE)ST.1943-541X.0001680

Xu, K., Bi, K., Han, Q., Li, X. and Du, X. (2019), "Using tuned mass damper inerter to mitigate vortex-induced vibration of long-span bridges: Analytical study", *Eng. Struct.*, **182**, 101-111. https://doi.org/10.1016/j.engstruct.2018.12.067

Zhang, R., Zhao, Z. and Dai, K. (2019), "Seismic response mitigation of a wind turbine tower using a tuned parallel inerter mass system", *Eng. Struct.*, **180**, 29-39. https://doi.org/10.1016/j.engstruct.2018.11.020

Zuo, H., Bi, K. and Hao, H. (2017), "Using multiple tuned mass dampers to control offshore wind turbine vibrations under multiple hazards", *Eng. Struct.*, **141**, 303-315. https://doi.org/10.1016/j.engstruct.2017.03.006

BS